Influence of pore property and alkalinity on the bio-deposition treatment efficiency of recycled aggregates

Wang, Jianyun; Zhang, Rui; Hou, Fuxing; Ye, Guang

DOI
10.1016/j.jobe.2024.109381

Publication date
2024

Document Version
Final published version

Published in
Journal of Building Engineering

Citation (APA)
Wang, J., Zhang, R., Hou, F., & Ye, G. (2024). Influence of pore property and alkalinity on the bio-deposition treatment efficiency of recycled aggregates. *Journal of Building Engineering*, *89*, Article 109381. https://doi.org/10.1016/j.jobe.2024.109381

Journal of Building Engineering 89 (2024) 109381

Contents lists available at ScienceDirect

Journal of Building Engineering

journal homepage: www.elsevier.com/locate/jobe

Influence of pore property and alkalinity on the bio-deposition treatment efficiency of recycled aggregates

Jianyun Wang [a,*], Rui Zhang [a], Fuxing Hou [a], Guang Ye [b]

[a] Department of Civil Engineering, School of Human Settlements and Civil Engineering, Xi'an Jiaotong University, Xi'an, 710049, China
[b] Department of Materials, Mechanics, Management & Design, Faculty of Civil Engineering and Geoscience, Delft University of Technology, Delft, the Netherlands

ARTICLE INFO

Keywords:
Recycled aggregates
Microbial induced carbonate precipitation (MICP)
Alkalinity
Pore structure
Sodium alginate

ABSTRACT

Microbial induced calcium carbonate precipitation (MICP) technology has been successfully used to enhance the properties of recycled concrete aggregates. However, the complex source and varied physical and chemical properties of recycled aggregates may have influence on the modification efficiency since microbes are often sensitive to the surroundings. In this study, two representative types of recycled aggregates, recycled concrete aggregates (RCA) and recycled brick aggregates (RBA), were subjected to two kinds of MICP treatments, basic MICP treatment and sodium alginate (SA) aided MICP treatment. The absorption and desorption of bacteria in/on aggregates during MICP treatments were quantified. The physical and chemical properties of aggregates after the bio-treatments were tested, and the influence of alkalinity and pore structure of aggregates under various MICP treatment methods on treatment efficiency were detailed investigated. Results indicated that, when the aggregates were subjected to the basic MICP treatment, the treatment efficiency was more remarkable in RBA, because of its high porosity and moderate pH (around 8–9), which facilitated the absorption of bacteria in/on aggregates and urease activity respectively. While under SA-aided MICP treatment, the influence of pore structure and alkalinity of aggregates on the treatment efficiency was not significant compared with that under the basic MICP treatment, especially the mass of $CaCO_3$ on the aggregates. The biogenic $CaCO_3$ generated by SA-aided MICP treatment not only plugged micropores, but also distributed all over the entire surface of the aggregates, resulting in a sufficient repair of microcracks. Meanwhile, the surface repair may reduce the influence of pore structure and pH of aggregates on the precipitation process, thereby reducing the impact of varied physical and chemical properties of aggregates on the treatment efficiency, which was conducive to the widely unified application of SA-aided MICP treatment in the modification of recycled aggregate based on construction solid waste.

1. Introduction

Construction and demolishing waste (CDW), which account for almost half of the world's solid waste, can be recycled as a sustainable and friendly source of building materials [1]. The demand for recycled aggregates is growing worldwide and is expected to increase from 45 billion tons in 2017 to 66 billion tons in 2025 [2]. However, the old attached mortar on the surface of recycled

* Corresponding author.
E-mail address: jianyun.wang@xjtu.edu.cn (J. Wang).

https://doi.org/10.1016/j.jobe.2024.109381
Received 20 January 2024; Received in revised form 3 April 2024; Accepted 16 April 2024
Available online 18 April 2024

aggregates contains many pores and microcracks, resulting in high porosity and low strength of recycled aggregates [3–5], which seriously influences the workability, the mechanical performance and durability of recycled concrete [6–8]. Therefore, many interesting methods such as physical grinding [9,10], microwave heating [11,12], and acid soaking [13–15], carbonation and nano-silica [16,17] were applied to modify recycled aggregates. All these methods could the properties of recycled aggregates, however they also come with additional costs and risks, for instance energy consumption, introduction of corrosive ions, and low compatibility with concrete. An environment-friendly and compatible method, Microbial Induced Carbonate Precipitation (MICP), is appropriate for enhancing the properties of recycled aggregates [18].

The purpose of MICP treatment of recycled aggregates is to plug pores and repair micro-cracks by use of the bacterially induced carbonate precipitation. One most often used strategy is an immersion-based MICP treatment, which has been demonstrated to be one of the most efficient way to enhance the properties of recycled aggregates [19]. Generally, the first step of the immersion-based MICP treatment is to allow bacterial cells to be absorbed on/into the pores of the aggregates, and in the second step, the aggregates with cells absorbed were transferred into a deposition solution consisting of precipitation precursors. The bacteria absorbed in the aggregates then start to induce the precipitation of biogenic $CaCO_3$ [19,20]. It can be seen that the MICP treatment efficiency greatly replies on the number of bacteria in/on the aggregates during the deposition process, which directly determines the precipitated amount of biogenic $CaCO_3$ in/on aggregates. Thus, the absorptive number of bacteria in/on aggregates in the first step, as well as the desorption rate of bacteria into solution phase in the second step, were especially crucial to influence the final treatment efficiency. Therefore, the pore structure of recycled aggregates has an impact on the treatment efficiency, because it directly influences the adsorption and desorption of bacteria in/on aggregates. Meanwhile, the urease activity of bacteria are often sensitive to the surroundings, such as alkalinity in the deposition process [21]. Therefore, recycled aggregates with various pore structure and alkalinity have great influence on the MICP treatment efficiency.

In practical applications, the recycled concrete aggregates (RCA) and recycled brick aggregates (RBA) are more common and required to be modified due to the old mortar on RCA and high porosity of RBA. Moreover, the MICP treatment efficiencies of RCA and RBA vary significantly. It was found in Wang's research [22] that the decrease of water absorption of RCA was around 9.1 % under the optimized immersion treatment, which was significantly lower than that of RMA (recycled mixed aggregates of RCA and RBA), about 25 %. In Liu's research [23], it was found that the mass increase due to the precipitates on RCA (2.5 %) was obviously lower than that on RBA (5.1 %), which had a discrepant influence on treatment efficiency due to the different physical and chemical properties between RCA and RBA. Therefore, it is important to investigate the effect of pore structure and alkalinity of aggregates on MICP treatment efficiency and to optimize the treatment methodology to obtain the highest treatment efficiency.

The commonly used immersion-based MICP treatment (referred to basic MICP treatment as follows) allows the bacterial cells to be physically absorbed in/on pores of the aggregates in the first step. However, when the bacteria containing aggregates are transferred into the deposition solution (with precipitation precursors) in the second step, the cells easily released from the open pores into the solution, resulting in less in-situ precipitation of biogenic $CaCO_3$ on the aggregates. And most of the precipitates are therefore formed on the upper surface of the aggregates due to gravity effect, while few amount were on the side and bottom surface of the aggregates. The uneven deposition weakens the modification effect. Thus, in our previous research [24], sodium alginate (SA) was innovatively used to firmly 'fix' cells on the full surface of the aggregates. In the first step, the aggregates were immersed in the mixture of SA and bacterial solution, and then transferred into a deposition solution (containing equimolar calcium nitrate and urea) in the second step, so the network structure of Ca-alginate was rapidly formed, and the bacterial cells were evenly coated on the aggregates. The cells act as nucleation sites of biogenic $CaCO_3$, and the homogeneous precipitates on the entire surface of the aggregates was thus obtained. The treatment efficiency was significantly improved.

In this study, to investigate the influence of pore structure and alkalinity of recycled aggregates on MICP treatment efficiency, two

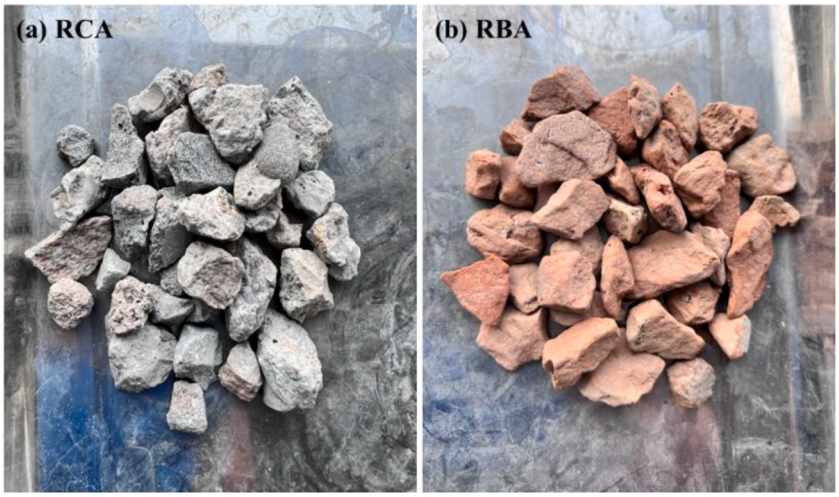

Fig. 1. Appearances of (a) RCA and (b) RBA

types of aggregates, RCA and RBA, which had different pore structure and alkalinity were used. Firstly, the absorption of bacteria in/on aggregates during the first step and the desorption of bacteria in saline and calcium solutions was measured, respectively. After that, the basic MICP treatment and SA-aided MICP treatment were applied to modify these two types of aggregates, and the treatment efficiency was evaluated in terms of the amount of biogenic precipitates and the decrease in water absorption of aggregates. In addition, the XRD, TGA, and SEM were applied to characterize the biogenic precipitates, and the MIP was used for characterizing the porosity and pores structure of RCA and RBA before and after MICP treatments.

2. Materials and methods

2.1. Recycled aggregates

As shown in Fig. 1, two different recycled aggregates, recycled concrete aggregate (RCA) and recycled brick aggregate (RBA), were used in this study, which were from a local factory in Xi'an, Shaanxi Province. The particle size (10–20 mm) of aggregates were sieved and used in this research. The physical properties, including apparent density and mass density, were tested according to BS EN 2002 [25]. The apparent density of RCA and RBA were 2620 kg/m^3 and 2520 kg/m^3, respectively; and the mass density of RCA and RBA were 1810 kg/m^3 and 1560 kg/m^3, respectively. The chemical compositions of RCA and RBA, as shown in Table 1, were tested by X-ray fluorescence (Bruker S8 Tiger, XRF)

2.2. Bacterial cultivation

A ureolytic bacterial strain, *Bacillus sphaericus* LMG 22257, was used for this research. The growth medium (abbreviated as UYE medium) containing urea (20 g/L) and yeast extract (20 g/L) was used, and the pH was adjusted to 8.5 under sterile conditions using 1 M NaOH or HCl solutions. The bacteria were cultivated in UYE medium (28 °C, 130 rpm) for 24 h, and then the bacterial solution was obtained. Subsequently, the bacterial pellets were harvested by centrifuging (7000 rpm, 10 min) the bacterial solution and the pellets were resuspended in the same volume of NaCl solution (8.5 g/L). The final concentration of pellet solution was around 5.4×10^7 cells/mL, which was used in the following experiments.

2.3. MICP treatments of different recycled aggregates

As shown in Table 2, two different recycled aggregates, RCA and RBA, were subjected to two types of MICP treatments, respectively. One was the basic MICP treatment [20] shown in Fig. 2(a). Step 1, the pellet solution was mixed with de-ionized water following a volume ratio of 1:1, the final concentration of pellet solution was 2.7×10^7 cells/mL. And then, the recycled aggregates (100 g) were fully immersed in the above pellet solution (100 mL) for 12 h to make the aggregates absorb enough bacteria. Step 2, the aggregates were taken out and transferred into the deposition solution (100 mL, 0.5 M) consisting of 0.5 M urea and 0.5 M Ca-nitrate for 7 d. The other type of the treatment was the SA-aided MICP treatment [26] shown in Fig. 2(b). Step 1, the pellet solution was mixed with 0.4 wt % SA solution following a volume ratio of 1:1, and the final concentration of SA and bacteria in the mixture were 0.2 wt% and 2.7×10^7 cells/mL, respectively. And then the aggregates were immersed into the bacterial pellets-SA mixture (100 mL) for 60 s to ensure that the surfaces were fully wrapped with a super thin layer of mixture. Step 2, the aggregates were taken out and completely submersed into the deposition solution (100 mL, 0.5 M) for 7 d. These groups were abbreviated as RCA-Basic group, RCA-SA group, RBA-Basic group, and RBA-SA group, as shown in Table 2. Nine replicates were performed for each group during step 1, three replicates of which were used in the step 2 and six replicates were used for the next absorption-desorption experiment. The treatment was carried out at room temperature.

Meanwhile, two control groups were performed on RCA and RBA, respectively, which were abbreviated as RCA-Control and RBA-Control in Table 2. The aggregates (100 g) were immersed in deposition solution (100 mL, 0.5 M) during the whole treatment process, approximately 7.5 d. The treatment process for the control group was also carried out at room temperature. The purpose of the control group was to examine the impact of the whole immersing treatment process on the mass change of the recycled aggregates, as well as the effect of calcium nitrate solution on the final biogenic precipitates. In previous study [26], the mass of the aggregates after the same treatment of control group showed a slight increase, which might be from calcium carbonate formed by the dissolution of CO_2 from the air into the calcium ion solution. Three replicates were conducted for each control group.

2.3.1. Absorption of bacteria in/on aggregates

The absorption of bacteria in/on aggregates of RCA-Basic group, RCA-SA group, RBA-Basic group, and RBA-SA group were tested by measuring the volume and concentration differences of the immersing solution between before and after absorption phase. The above six replicates were applied for measuring the absorption of bacteria in/on aggregates during step 1. As shown in Fig. 3, before immersing the aggregates (step 1 in Fig. 2), the volume (V1, mL) and concentration (C1, cells/mL) of the pellets solution/mixture of pellets and SA were measured by a cylinder and UV spectrophotometry, respectively. After 12 h, the aggregates were taken out, then three replicates were transferred into saline solution and three replicates were transferred into calcium nitrate solution (0.5 M) in the

Table 1
Chemical compositions (wt%) of recycled concrete aggregates.

	SiO_2	Na_2O	Al_2O_3	CaO	MgO	Fe_2O_3	K_2O
RCA	44.3	21.0	17.2	8.8	6.5	0.6	1.2
RBA	49.1	15.0	19.8	4.0	8.1	1.8	1.2

Table 2
Experiments of different MICP treatments on different recycled aggregates.

Abbreviation of each group	Aggregates	MICP treatment
RCA-Control	RCA	Control
RCA-Basic	RCA	Basic
RCA-SA	RCA	SA-aided
RBA-Contro	lRBA	Control
RBA-Basic	RBA	Basic
RBA-SA	RBA	SA-aided

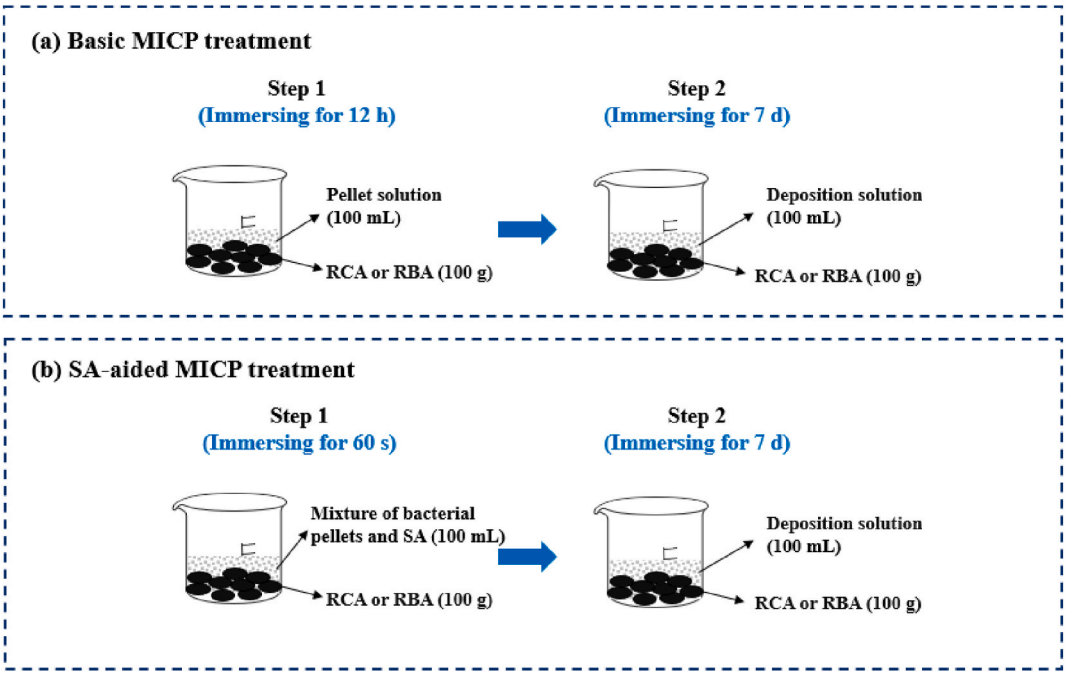

Fig. 2. Diagram of (a) Basic MICP treatment and (b) SA-aided MICP treatment.

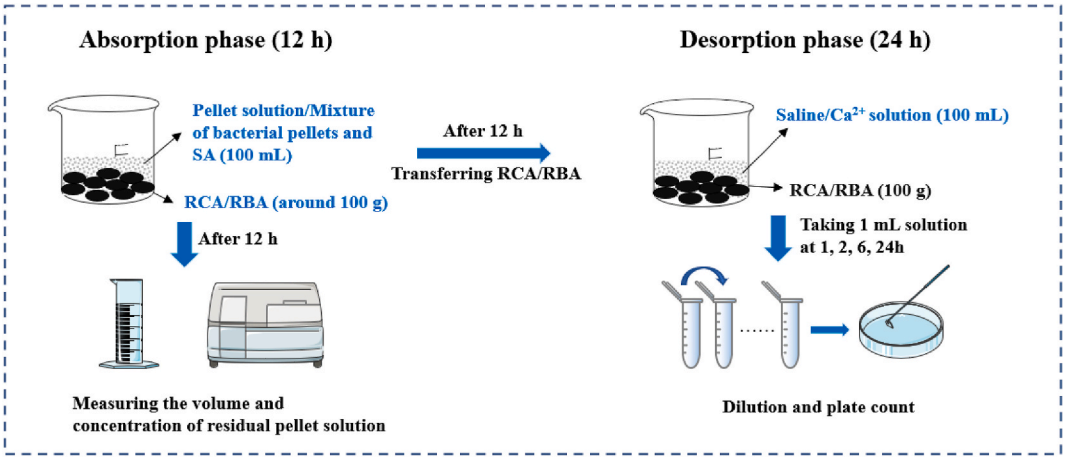

Fig. 3. Diagram of absorption and desorption of bacteria in/on aggregates.

next experiment, respectively. The volume (V2, mL) and concentration (C2, cells/mL) of the residual pellet solution were measured and calculated again. The absorption rate can be represented by Eq. (1).

$$Absorption\ rate\ (cells/g) = \frac{V1 \times C1 - V2 \times C2}{aggregates\ (g)} \tag{1}$$

2.3.2. Desorption of bacteria in/on aggregates

The dynamic desorption in the saline/Ca^{2+} solution of bacteria from RCA-Basic group, RCA-A group, RBA-Basic group, and RBA-SA group were obtained by measuring the number of bacteria released from the aggregates, which was determined by the plate counting method. In the desorption phase, two immersing solutions, saline solution and calcium nitrate solution (0.5 M), were applied and the above six replicates were used. Three replicates were immersed in saline solution and three replicates were immersed in the Ca^{2+} solution. The aggregates with fully absorbed bacteria were transferred into saline solution, which can clearly reflect the effect of the aggregates themselves on the adhesion of bacteria without the disturbance of Ca^{2+}, therefore the impact of pore structure and alkalinity on the desorption of bacteria could be examined. Transferring into the Ca^{2+} solution could simulate the desorption of bacteria during the process of biological deposition. Many studies have found that calcium ions affect bacterial urease activity. For instance, previous research discovered that at a bacterial concentration of 10^7 cells/mL, calcium ion showed an inhibitory effect on bacterial urease activity. Urease activity was higher in 0.25 M Ca^{2+} solution than that in 0.5 M Ca^{2+} solution [21]. Therefore, in the real bio-deposition treatment condition (0.5 M Ca^{2+} solution), the detected desorption of bacteria could be lower than that in a saline solution. As shown in Figs. 3 and 1 mL of immersion solution was taken out at 1, 2, 6, 24 h for plate counting. The counting was the desorbed bacterial cells at that time, and the desorption rate can be calculated by Eq. (2). To conduct plate counts for each group, serial dilutions from 10-fold to 10^6-fold were measured to ensure a countable number of bacterial colonies formed on the plate. Plates with final colony counts between 30 and 300 were considered as the valid result. The dilution steps in this experiment were precise, and multiple parallel count samples (n = 3) were used for each sampling to increase the reliability of the results.

In addition, the pellet solution (100 mL, three replicates) was placed in the room environment during the whole desorption process as the reference group, the initial and final concentrations of bacteria were measured to calculate the naturally degradation during the whole absorption and desorption process.

$$Desorption\ rate\ (\%) = \frac{desorbed\ bacteria\ (cells)}{absorbed\ bacteria\ (cells)} \times 100\% \tag{2}$$

2.4. Efficiency of MICP treatments

2.4.1. Urea decomposition and pH evolution during the deposition process

The precipitation process of the MICP treatment was monitored by the urea decomposed and pH evolution. The urea decomposed (mmol/L) and urea decomposition efficiency (%) were calculated by Eqs. (3) and (4) [24]. One mole of urea is decomposed into 1 mol of carbonate ions and 2 mol of ammonium nitrogen. The ammonium nitrogen was measured by a Nessler's method (TAN) [27]. Samples (3 mL) were taken. Around 1 ml was filtered to remove the cells and maybe precipitates before applying the TAN method. The rest of the samples (around 2 mL) were taken for the measurement of pH value (BPH-7100). The concentration of ammonia nitrogen and pH were tested at 2 h, 6 h, 10 h, 1 d, 2 d, 3 d, 4 d, 5 d, 6 d, and 7 d, respectively.

$$urea\ decompsed\ (mmol/L) = \frac{N - NH_4^+(mg/L) \times 60(g/mol)}{2 \times 14\ (g/mol) \times 60(g/mol)} \tag{3}$$

$$urea\ decomposition\ efficiency\ (\%) = \frac{urea\ decompsition\ (mmol/L) \times 10^{-3}}{0.5\ (mol/L)} \times 100\% \tag{4}$$

2.4.2. Visualization of the surface of the treated-aggregates

After MICP treatment, the appearance of RCA and RBA was photographed by a camera (Canon PowerShot G7), which showed the distribution of biogenic precipitates on RCA and RBA.

2.4.3. Mass increase of the treated aggregates

After MICP treatment, the mass increase of aggregates was mainly due to the formed biogenic precipitates, which directly reflected the efficiency of the MICP treatment. The following Eq. (5) was used to calculate the mass increase of the treated aggregates. All of masses were weighed after drying in a 40 °C oven till obtaining a stable value.

$$Mass\ increase\ (\%) = \frac{M_2 - M_1}{M_1} \times 100\% \tag{5}$$

Where: M_1 was the mass of aggregates before MICP treatment, g; M_2 was the mass of aggregates after MICP treatment, g.

2.4.4. X-ray diffraction analysis

The mineral composition of biogenic precipitates on RCA and RBA were qualitatively detected by X-ray diffraction (XRD, Bruker D8 ADVANC). Before the test, the biogenic precipitates generated on the dried aggregates after MICP treatment were ground into the powder of around 200 mesh in porcelain mortar and uniformly mixed. The powder was made into samples with a flat surface for scanning. The scanning step size was 0.02° and the scanning range was 20–70°.

2.4.5. Thermogravimetric analysis

Thermogravimetric analysis (TGA) was used to detect the formation of the biogenic precipitates. The preparation of sample powder was the same as the XRD test. The samples placed on the sample stage of the instrument (METTLER TOLEDO TGA/DSC3+). The temperature of powder sample was raised from room temperature to 1000 °C at a rate of 10 °C/min under nitrogen. The mass loss of the sample during heating was recorded and displayed in a mass-temperature graph.

2.4.6. Decrease in water absorption of aggregates

The decrease of water absorption of aggregates could evaluate the efficiency of MICP treatment. The water absorptions of recycled aggregates before and after treatment (WA_{before} and WA_{after}) were measured according to BS EN 2002 [25]. The following Eq. (6) was applied to calculate the decrease of water absorption of aggregates. WA decrease was the decrease of water absorption of aggregates after treatment. WA_{before} was the water absorption of aggregates before treatment (%). WA_{after} was the water absorption of aggregates after treatment (%).

$$WA\ decrease\ (\%) = \frac{WA_{before} - WA_{after}}{WA_{before}} \times 100\% \tag{6}$$

2.4.7. Morphology of the surface of aggregates

Scanning electron microscopy (SEM, ZEISS GEMINI 500) was applied to observe the morphology of the untreated and bio-treated aggregates under an accelerating voltage of 10 kV. The surface of aggregate was coated with gold before testing. Meanwhile, the element compositions of different aggregates were determined by an energy dispersive spectrometer (Oxford EDS System).

2.4.8. Pore size distribution and porosity

The pore size distribution and porosity of recycled aggregates before and after MICP treatments were characterized by a mercury intrusion porosimetry (MIP, Autopore IV 9500). In this study, the ambient temperature was 19 °C, the pressure range was 0.2–60000 psi, and the pore size range was 800 μm to 3 nm.

3. Results and discussion

3.1. Absorption of bacteria in/on aggregates

The absorption rate represents the actual adhesion of bacterial cells number in/to the aggregates. As shown in Fig. 4, under the basic MICP treatment, the absorption rate of bacteria in RCA-Basic group was 5.63×10^6 cells/g on average, which was only about half as much as that of RBA-Basic group, 1.11×10^7 cells/g on average. Under same SA-aided MICP treatment, the absorption rate of bacteria was 1.13×10^7 cells/g on average in RCA-SA group. For RBA, the absorption rate of bacteria was 1.76×10^7 cells/g on average in RBA-SA group, which was about 56 % higher than that of RCA-SA group. The significant improvement of absorption rate of bacteria in/on RBA, comparing with RCA, might be due to the different of pore properties between them. The porosity of RBA is normally higher than that of RCA, and RBA contains more large pores. The more pores there were, the more bacteria could be adsorbed and retained, and larger pores allowed bacteria to be adsorbed and retained more quickly within the pores. Therefore, the high porosity and the larger number of large pores in RBA resulted in a higher capacity to adsorb bacteria, in terms of both the quantity of bacteria adsorbed and the rate of adsorption, compared to RCA.

For the same aggregates, for instance RCA, the absorption rate of bacteria in RCA-Basic group (5.63×10^6 cells/g on average) was significantly lower than that in RCA-SA group (1.13×10^7 cells/g on average). This indicated that SA-aided MICP treatment can obtain almost twice the absorption of bacteria than that of basic MICP treatment on RCA. Regarding RBA, the absorption rate of bacteria in RCA-SA group (1.76×10^7 cells/g on average) was also significantly higher than that in RCA-Basic group (1.11×10^7 cells/g on average), which improved 59 % under SA-aided MICP treatment. This suggested that the viscous SA could promote more bacterial cells

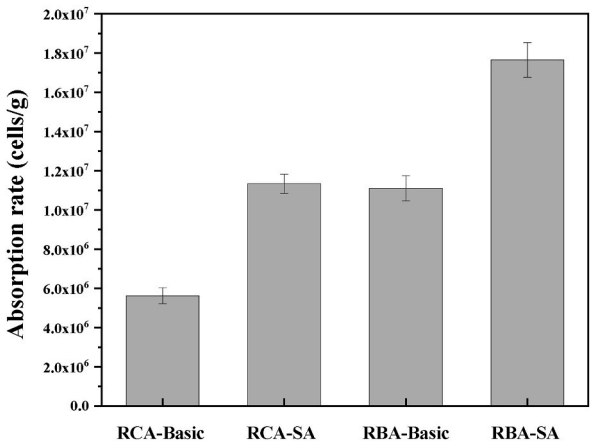

Fig. 4. Absorption of bacteria in/on aggregates.

to adhere to the aggregates.

3.2. Desorption of bacteria from the aggregates

The desorption rate of bacteria within 24 h directly indicated the release of the bacteria from the aggregates to the solution phase during the bio-deposition process. Theoretically, the optimal residence sites of the bacteria are the pores or the surface of aggregates, and the bacteria, as the nucleation sites, promote the biogenic $CaCO_3$ in-situ generated in/on the aggregates. Therefore, the fewer bacteria releasing into the solution phase, the more precipitates could form in-situ in/on the aggregates. The release of bacteria into the saline solution can indicate the adhesion property of different aggregates to bacteria under different MICP treatments, without the interference of Ca^{2+} to bacterial activity. As shown in Fig. 5, in the first hour, the desorption rate of bacteria from the aggregates rose sharply, reaching 76.7 % in RCA-Basic group, 46.2 % in RCA-SA group, 71.4 % in RBA-Basic group, and 46.6 % in RBA-SA group. At 2 h, the desorption rate continued to increase, and reaching 87.7 % in RCA-Basic group, 72.4 % in RCA-SA group, 72.8 % in RBA-Basic group, and 65.1 % in RBA-SA group. At 6 h, the increase of desorption rate was apparently slow, only reaching 88.3 % in RCA-Basic group, 80.6 % in RCA-SA group, 81.9 % in RBA-Basic group, and 70.7 % in RBA-SA group. This could be found that for the RCA-Basic group and RBA-Basic group, the desorption rate of bacteria at 1 h almost reached their highest value. For the RCA-SA group and RBA-SA group, from 1 h, the desorption rate increased rapidly and almost reached the highest value till 2 h. And after that, the desorption rate of bacteria in all groups increased slowly and reached the highest value at 24 h, 90.6 % in RCA-Basic group, 86.6 % in RCA-SA group, 88.9 % in RBA-Basic group, and 76.3 % in RBA-SA group. It was illustrated that for RCA-Basic group and RBA-Basic group, it took around 1 h for bacteria almost completely to escape into external saline solution. And for RCA-SA group and RBA-SA group, it would take 2 h. This difference indicated that most bacteria do not stay longer than 1 h in/on aggregates, relying solely on their physical adhesion to the aggregates. Adding sticky SA helped the bacteria stick to the aggregates longer, but only for 2 h.

At 24h, it can be seen in Fig. 5 that the final bacterial desorption rate reached to maximum 90.6 % of RCA-Basic group. Also for the reference group, the concentration of pellet solution (100 mL) decreased from 5.4×10^7 cells/mL to 5.1×10^7 cells/mL, indicating that the concentration of pellets degraded to 94.4 % within 24h. It can be calculated that only approximately 3.8 % of bacteria stayed in/on the aggregates, which means that almost all precipitates would form in the solution phase instead of in/on the aggregates, and then fell down on the top surface of aggregates due to gravity effect. Thus only top surface was covered by the precipitates, and other surfaces were barely covered [24]. As for RCA-SA group, it can be found that the bacterial desorption rate was lower than RCA-Basic group at all times, at 2 h, the former (72.4 % on average) was apparently around 80 % of the latter (87.7 % on average). This further indicated that the viscosity of SA could facilitate bacteria to adhere to aggregates. As the immersing time in saline solution, more bacteria were gradually desorbed to solution phase, and the final bacterial desorption rate of RCA-SA group reach to 86.6 % on average. This was because SA merely sticked the bacterial cells on the aggregates, rather than fixing the cells on aggregates. While in the actual deposition process, the network structure of Ca-alginate would rapidly form when SA was exposed to Ca^{2+} (in step 2), which has a firm fixation effect on bacteria.

Similar results were found in the RBA-Basic and RBA-SA groups, the bacterial desorption rate rose to 88.9 % and 76.3 % on average at 24 h, respectively. Under same MICP treatments, the desorption rates of RCA were higher than that of RBA. It might be due to the more suitable pH (around 8–9) and higher porosity of RBA, which was more conducive to the retention of more bacteria in/on the aggregates.

Fig. 6 shows the desorption of bacteria from the aggregates in the Ca^{2+} solution. It could illustrate the bacterial release in the real treatment process since during the step 2 of MICP treatment, the aggregates would be immersed in the deposition solution containing calcium nitrate. Under basic MICP treatment, in the first 2 h, the desorption of bacteria in RCA-Basic group and RBA-Basic group increased most rapidly, reaching 55.0 % and 51.2 % on average at 2 h, respectively. At 6 h, the desorption of bacteria in RCA-Basic group and RBA-Basic group grew more slowly, reaching 56.3 % and 53.6 % on average, respectively. And then, the final desorption of bacteria in RCA-Basic group and RBA-Basic group were 74.6 % and 70.7 % on average, respectively. Under SA-aided MICP treatment,

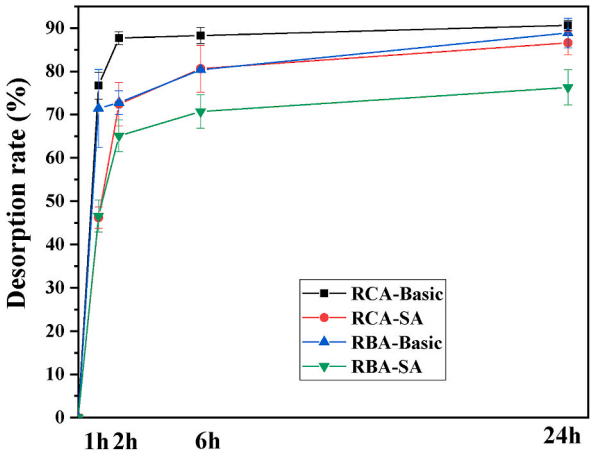

Fig. 5. Desorption of bacteria from aggregates in saline solution.

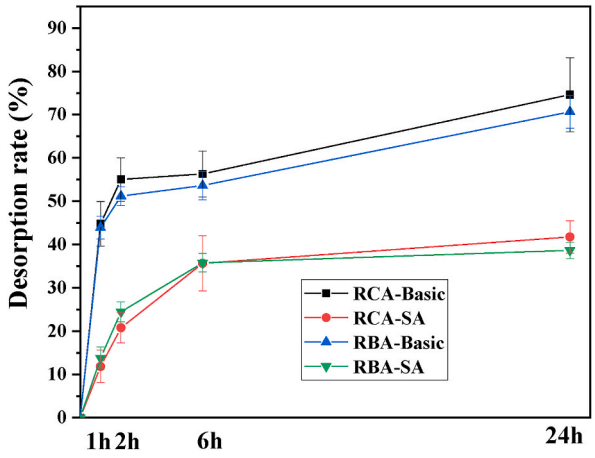

Fig. 6. Desorption of bacteria from aggregates in Ca^{2+} solution.

before 6 h, the desorption of bacteria in RCA-SA group and RBA-SA group have been rising significantly until reaching 35.7 % and 35.8 % on average at 6 h, respectively. Subsequently, the desorption of bacteria in RCA-SA group and RBA-SA group increased slowly, reaching 41.8 % and 38.6 % on average at 24 h, respectively. It was found that under same MICP treatment, the desorption of bacteria maintained the same increase rate regardless of RCA and RBA, indicating the desorption trend of bacteria remained the same. While the desorption of bacteria in RCA groups always slightly higher than that in RBA groups, which might be that the bacteria were inclined to stay in the larger pores of RBA and penetrate into deeper pores inside of RBA, thus they were comparatively not readily to desorb from aggregates.

For RCA, the desorption of bacteria in RCA-SA group was significantly lower than that in RCA-Basic group at all times. The final desorption rate of bacteria in RCA-Basic group (74.6 % on average) was around 78 % higher than that in RCA-SA group (41.8 % on average). For RBA, the desorption of bacteria in RBA-SA group was also significantly lower than that in RBA-Basic group at all times. This was due to the fact that when SA exposed to Ca^{2+}, the network structure of Ca-alginate would formed instantly on aggregates, which played a crucial role in entrapping bacterial cells [26]. This prevented many bacteria from releasing into solution. For example, at 2 h, the desorption rate of RCA-Basic group and RBA-Basic group reached to 55.0 % and 51.2 % on average, respectively, which were much higher than the RCA-SA and RBA-SA groups, 20.8 % and 24.5 % on average. This further indicated that the Ca-alginate formed quickly and prevented around half of bacteria from releasing into solution phase.

In Fig. 6, at 1 h, the desorption rate of bacteria from the aggregates in Ca^{2+} solution apparently increased, only reaching 44.8 % in RCA-Basic group, 11.8 % in RCA-SA group, 43.9 % in RBA-Basic group, and 13.8 % in RBA-SA group, which were significantly lower than that in saline solution shown in Fig. 5. And then the desorption rate gradually increased until 6 h, reaching 56.3 % in RCA-Basic group, 35.7 % in RCA-SA group, 53.6 % in RBA-Basic group, and 35.8 % in RBA-SA group. The difference with the desorption of bacteria in saline solution in Fig. 5 was that, in Ca^{2+} solution, the desorption rate reached to a stable state at 6 h in RBA-Basic group and RBA-SA group, even at 24 h in RCA-Basic group and RCA-SA group. And the final desorption rate in RCA-Basic group, RCA-SA group,

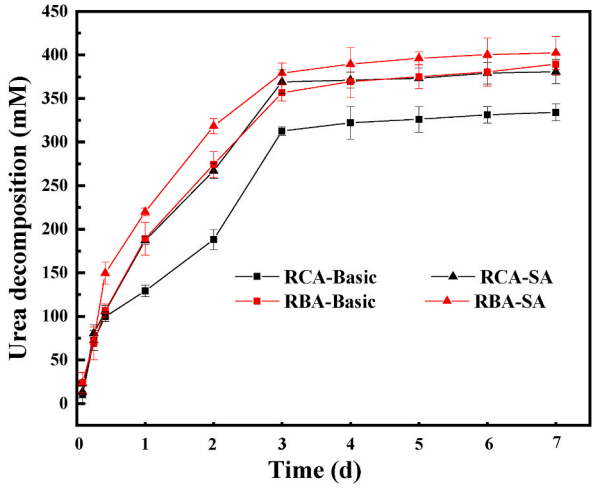

Fig. 7. The urea decomposition of different recycled aggregates under basic and SA-aided MICP treatments.

RBA-Basic group, and RBA-SA group were only 74.6 %, 41.8 %, 70.7 %, and 38.6 % on average, respectively. While in saline solution, the desorption of bacteria in all groups reached to a stable state at 1h and at the latest at 2 h. The final desorption rate in RCA-Basic group, RCA-SA group, RBA-Basic group, and RBA-SA group were 90.6 %, 88,9 %, 86.6 %, and 76.3 % on average, respectively. The reason might be that, for basic MICP treatment, Ca^{2+} might have a negative effect on bacterial activity. For SA-aided MICP treatment, the network of Ca-alginate prevented the bacteria from releasing into solution phase. As a result, it can be seen that the release of bacteria in RCA-Basic group and RBA-Basic group in Fig. 6 were much more durable and had a much lower final desorption rate than that of Fig. 5.

3.3. Urea decomposition and pH evolution during deposition process

The formulas of bio-precipitation process were shown in Eqs. (7) and (8). As shown in Eq. (7), the decomposition of urea depends on the bacterial urease activity. With the presence of Ca^{2+}, the formed CO_3^{2-} immediately react with Ca^{2+} to generate biogenic $CaCO_3$, as shown in Eq. (8). Therefore, the formation rate of biogenic $CaCO_3$, is closely related to the urea decomposition rate. In Fig. 7, in the first 3 d, the urea decomposition rate was the fastest, and after 3 d, the urea decomposition hardly increased, which indicated that the deposition reaction mainly occurred within the first 3 d. This was consistent with the findings of previous studies [26,28].

$$CO(NH_2)_2 + 2H_2O \xrightarrow{Bacterial\ urease} 2NH_4^+ + CO_3^{2-} \tag{7}$$

$$CO_3^{2-} + Ca^{2+} \rightarrow CaCO_3 \downarrow \tag{8}$$

Under basic MICP treatment, the urea decomposition in RCA-Basic group was lower than that in RBA-Basic group from 1 d to 7 d. The reason might be that the higher porosity and more suitable alkalinity of RBA absorbed more bacteria to promote the decomposition of urea. In the first 3 d, the urea decomposition in RCA-Basic group and RBA-Basic group increased rapidly, reaching at 313 mM and 356 mM on average, respectively. After 3 d, the increase of urea decomposition in RCA-Basic group and RBA-Basic were gradually slow, and the final urea decomposition reached to 334 mM and 389 mM on average, respectively. It indicated that most urea was decomposed within 3 d. Under SA-aided MICP treatment, the urea decomposition in RCA-SA group was also lower than that in RBA-SA group. Similarly, in the first 3 d, the growth of urea decomposition was rapid, and after 3 d, the growth of urea decomposition in RCA-SA group and RBA-SA group gradually stabilized, and the final urea decomposition reached to 381 mM and 402 mM on average, respectively. For RCA, the urea decomposition in RCA-SA group was significantly higher than that in RCA-Basic group at all times, which might be that the network structure of Ca-alginate encapsulated more bacteria, and promoting the decomposition of urea. For RBA, the urea decomposition in RBA-SA group was similarly higher than that in RBA-Basic group at all times.

The amount of bacteria absorbed in/on aggregates in the first step is the crucial factor to influence the urea decomposition in solution. In Fig. 4, it was shown that the absorption of bacteria was 5.63×10^6 cells/g in RCA-Basic group, 1.13×10^7 cells/g in RCA-SA group, 1.11×10^7 cells/g in RBA-Basic group, and 1.76×10^7 cells/g in RBA-SA group. It was observed that the decomposition rate in RBA groups were higher than that in RCA groups from the beginning to end under same MICP treatment. The reason could be that the physical and chemical characteristics of RBA had a positive effect on the bacterial activity urease, which would be discussed in detail as follows.

Under the basic MICP treatment, for the different aggregates, it could be calculated that the absorption of bacteria in RBA-Basic group was around 2 times more than that in RCA-Basic group. Accordingly, in Fig. 7, at 1 d, the urea decomposition in RCA-Basic group and RBA-Basic group were 129 mM and 189 mM on average, respectively. The difference in urea decomposition was from the fact that RBA absorbed more bacteria than RCA, which was conducive to the decomposition of urea in solution. The reason might be that RBA had higher porosity and a pH was more suitable for urease activity. At 3 d, the decomposition of urea continued to rise, reaching 313 mM in RCA-Basic group and 356 mM in RBA-Basic group, and at 7 d, the final decomposition of urea increased to 334 mM in RCA-Basic group and 389 mM in RBA-Basic group. It was found that the differences between RCA-Basic group and RBA-Basic group at 3 d and 7 d were less significant than that at 1 d, which indicated that, due to the higher absorption of bacteria in RBA-Basic group, the urea decomposition in RBA-Basic group was significantly higher than that in RCA-Basic group in the first 1 d. And the difference of urea decomposition between RCA-Basic group and RBA-Basic group decreased at 3 d and 7 d, which also indicated that the bacteria could continue to decompose urea after 1 d.

Under the SA-aided MICP treatment, it also could be calculated that the absorption of bacteria in RBA-SA group was 56 % higher than that in RCA-SA group. Correspondingly, in Fig, 7, at 1 d, the urea decomposition in RCA-SA group and RBA-SA group were 187 mM and 220 mM, respectively, which was caused by the fact that RBA absorbed more bacteria than RCA due to the higher porosity and more suitable pH of RBA. At 3 d, the urea decomposition in RCA-SA group and RBA-SA group were 369 mM and 379 mM, respectively. And at 7 d, the urea decomposition in RCA-SA group and RBA-SA group were 381 mM and 402 mM, respectively. It was found that the differences, such as absorption of urea and urea decomposition from different aggregates under SA-aided MICP treatment, were less significant than that under basic MICP treatment, which might be to promote SA-aided MICP treatment to reduce the differences in treatment efficiency caused by different aggregates.

Comparing the different MICP treatments, the urea deposition under SA-aided MICP treatment was correspondingly higher than that under basic MICP treatment at all times. According to the absorption rate of bacteria in Fig. 4, the adhered bacteria in/on aggregates under SA-aided MICP treatment were much more than that under basic MICP treatment. For example, the urea decomposition in RBA-Basic group and RBA-SA group were 189 mM and 220 mM, respectively, which was due to the fact that the absorption of bacteria in RBA-SA group was 72 % higher than that in RBA-Basic group. This indicated that Ca-alginate network produced by SA-aided ‘fixed’ more bacteria than that of basic MICP treatment. It can be foreseen that more bacteria can promote more

precipitation of biogenic precipitates [29].

It was well known that pH value is one of the important factors affecting bacterial urease activity and hence the precipitation of $CaCO_3$ [30]. Thus, the pH value of the deposition solution was monitored during the precipitating process. As shown in Fig. 8, the pH value in RCA-Control group was around 9 during the whole deposition process, which was higher than that in RBA-Control group (around 8), indicating that the initial pH of RCA was higher than that of RBA. At 3 d, the pH value of RCA-Basic group and RCA-SA group increased to 10.24 and 9.92 on average, respectively. Meanwhile, the pH value of RBA-Basic group and RBA-SA group increased to 8.99 and 8.93 on average, respectively. The rise in pH value was mainly due to the decomposition of urea catalyzed by bacterial urease and produced NH_3/NH_4^+.

In RCA-Basic group, the pH value increased from 9.02 to 10.27 on average after 7 d. And the pH value in RCA-SA group increased from 8.84 to 10.1 on average. For the RBA, the pH values increased from 8.03 to 9.15 on average in RBA-Basic group and from 7.92 to 9.16 on average in RBA-SA group. Combined the urea decomposition in Fig. 7, under same basic MICP treatment, the urea decomposition in RBA-Basic group was always higher than that in RCA-Basic group. And under same SA-aided MICP treatment, the urea decomposition in RBA-SA group was higher than that in RCA-SA group at all times. This might indicate that differences in the alkalinity of different aggregates caused differences in urea decomposition. Previous research has found that the optimal pH range for bacterial growth and spore germination of *Bacillus sphaericus* LMG 22257 was 7–9 [21]. Moreover, it has been noted that the optimal initial pH environment using the MICP method was 6.5–9.3 [31], and studies have shown that urease activity was significantly reduced under acidic (below pH 6) and alkaline (above pH 9) conditions [32]. This indicated that the alkalinity of RBA (around 8–9) has more positive effect on bacteria than that of RCA, thus producing higher urease activity to promote the decomposition of urea. Nevertheless, the high porosity of RBA is still the most significant factor influencing the urea decomposition. The more pores in the aggregates, the more bacteria could be absorbed (meaning the higher the urease activity), thus promoting the decomposition of more urea.

3.4. Visualization of the surface of the treated aggregates

Fig. 9 showed the appearance of RCA after basic and SA-aided MICP treatment. the aggregates treated by basic MICP treatment were shown in Fig. 9(a) and (b), obvious white precipitates were only found on the top surface of the aggregates, while almost no precipitates were found on the bottom surface. Differently, in Fig. 9(c), many white precipitates were found on the top surface of aggregates after SA-aided MICP treatment, and almost similar amount of precipitates were seen in Fig. 9(d) on the bottom surface. This was because under basic MICP treatment, the bacteria, acted as nucleation sites, were physically absorbed on aggregates. Yet, when the aggregates were transferred to the deposition solution, the bacteria were easily desorbed and released into the solution environment. This led to many biogenic precipitates to generate in the solution phase, thus only the top surface was covered with a layer of precipitates due to gravity. However, the top and bottom surface of RCA after SA-aided MICP treatment were almost covered by precipitates, which indicated that SA-aided MICP treatment prompted the precipitates in-situ generated on the aggregates. This was because, during the SA-aided treatment process, the viscous sodium alginate evenly 'glue' the bacteria onto the aggregates. When the sodium alginate contacts with calcium ions, a network structure of calcium alginate rapidly formed, which had a stronger capacity to encapsulate and fix the bacteria. This facilitated the bacteria acting as nucleation sites, promoting the in-situ formation of calcium carbonate on the aggregates. This was consistent with the conclusions of previous studies [24,26].

Similar phenomenon could be seen in Fig. 10, the coverage of the precipitates on RBA surface after SA-aided MICP treatment was much more than that after basic MICP treatment. In addition, it could be observed that the coverage of RBA surface also similar with that of RCA surface under SA-aided MICP treatment, and the amount of precipitates on RCA and RBA after SA-aided MICP treatment was intuitively difficult to compare, which indicated that SA-aided treatment method was widely appropriate for various aggregates and narrowed the difference in distribution of precipitates on different aggregates.

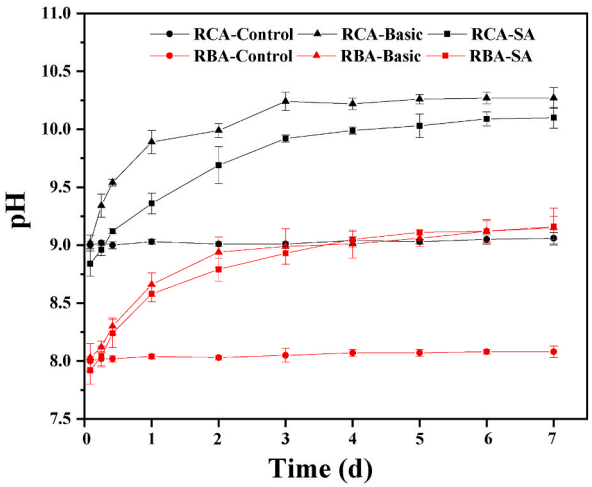

Fig. 8. The pH evolution of different recycled aggregates under basic and SA-aided MICP treatments.

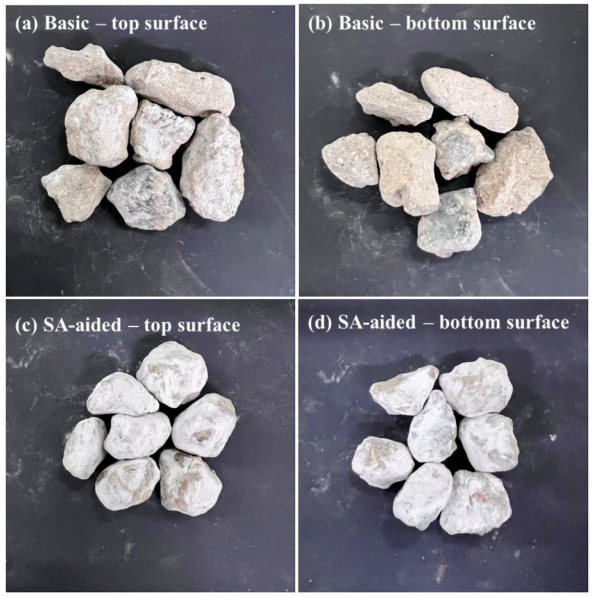

Fig. 9. The (a) top surface of RCA after basic MICP treatment, (b) bottom surface of RCA after basic MICP treatment, (c) top surface of RCA after SA-aided MICP treatment, and (d) bottom surface of RCA after SA-aided MICP treatment.

Fig. 10. The (a) top surface of RBA after basic MICP treatment, (b) bottom surface of RBA after basic MICP treatment, (c) top surface of RBA after SA-aided MICP treatment, and (d) bottom surface of RBA after SA-aided MICP treatment.

3.5. Mass increase of the treated aggregates

The mass increase of aggregates after the MICP treatments was due to the formation of biogenic precipitates, and the amount of biogenic precipitates were strongly related to the number of bacteria adhered in/on aggregates. As shown in Fig. 11, under same basic MICP treatment, the mass increase in RCA-Basic group was 3.94 % on average, which was lower than that in RBA-Basic group, 4.59 % on average. The absorption of bacteria in RBA-Basic group (1.11×10^7 cells/g on average) was twice as much as that in RCA-Basic group (6.63×10^6 cells/g on average). This directly resulted in that the final decomposition of urea in RBA-Basic group (389 mM on average) was around 16.5 % higher than that in RCA-basic group (334 mM on average) in Fig. 7. Therefore, the generated biogenic precipitates (mass increase) in RBA-Basic group were more than that in RCA-Basic group. Under same SA-aided MICP treatment, the mass increase in RCA-SA group was 4.53 % on average, which was slightly lower than that in RBA-SA group, 4.63 % on average. This was also related to the high porosity of RBA, which absorbed more bacteria and led to higher decomposition of urea.

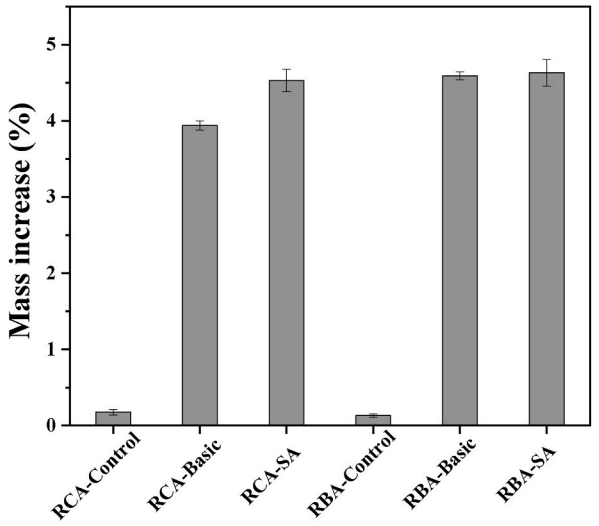

Fig. 11. The mass increase of different aggregates under different MICP treatments.

For RCA, the mass increase in RCA-SA group (4.53 % on average) was significantly higher than that in RCA-Basic group (3.94 % on average). This was due to that fact that the SA could absorb more bacteria in/on aggregates, and the quickly formed network structure of Ca-alginate in the initial time of deposition process could encapsulated more bacteria in-situ on the aggregates, which could be demonstrated by the absorption of bacteria in Fig. 4 and the desorption of bacteria in Ca^{2+} solution in Fig. 6. And more bacteria on aggregates led to a higher decomposition of urea, thus promoting the generation of biogenic precipitates. And for RBA, the mass increase in RBA-SA group (4.63 % on average) was slightly higher than that in RBA-Basic group (4.59 % on average), which also related to the viscidity of SA and the formed Ca-alginate in the deposition process.

In addition, it was found that in the difference in mass increase from different aggregates under SA-aided MICP treatment (4.53 % in RCA-SA group and 4.63 % in RBA-SA group) was apparently less significant than that under Basic MICP treatment (3.94 % in RCA-Basic group and 4.59 % in RBA-Basic group). And it was found that in Fig. 4 that compared with RBA and RCA, the increase of absorption of bacteria under SA-aided MICP treatment (about 56 % increase in RBA-SA group compared with RCA-SA group) was less significant than that under Basic MICP treatment (about 97 % increase in RBA-Basic group compared with RCA-Basic group). This resulted in that in Fig. 7, the difference of final decomposition of urea between RCA and RBA decreased due to SA-aided MICP treatment. Based on this, it could be indicated that SA-aided MICP treatment is conducive to narrow the influence from different aggregates on treatment efficiency.

3.6. Decrease in water absorption of aggregates

The decrease of water absorption of aggregates in Fig. 12 directly shows the efficiency of MICP treatment. The formed precipitates plugged the pores in aggregates, and resulting in the decrease of water absorption. Under the basic MICP treatment, the decrease in

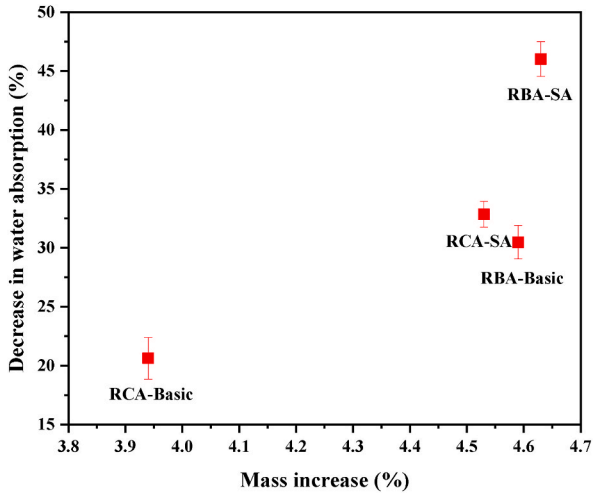

Fig. 12. The decrease of water absorption and increase of densities of different aggregates under different MICP treatments.

water absorption of aggregates in RBA-Basic group was 30.47 % on average, which was much higher than that in RCA-Basic group (20.63 % on average). Correspondingly, it could be found that the mass increase of treated aggregates in RBA-Basic group (4.59 % on average) was higher than that in RCA-Basic group (3.94 % on average). This difference in treatment efficiency was mainly caused by the difference in pore structure between RCA and RBA. Higher porosity of RBA could absorb more bacteria, and promoting the more urea decomposition, and forming more precipitates to repair pore, thus resulting in higher decrease in water absorption of aggregates. Moreover, the difference in alkalinity between RCA and RBA was also one of the important factors to influence the efficiency of MICP treatment, more suitable pH in RBA for bacterial urease activity could promote the decomposition of urea.

Under same SA-aided MICP treatment, it was also found that the decrease in water absorption of aggregates in RBA-SA group was 46.02 % on average, which was much higher than that in RCA-Basic group (32.85 % on average). While the mass increases of RBA-SA group and RCA-SA group were similar, 4.63 % and 4.53 %, respectively. It implied that more precipitates formed on aggregates did not represent a higher decrease in water absorption. This might be related to the distribution of precipitates in the pores of aggregates. The precipitates might be readily formed in the inner pores and large pores in RBA, not the small pores in RCA. The precipitates were only stacked on the surface of RCA, and this part of precipitates was invalid for the decrease in water absorption of aggregates. SA-aided MICP treatment could narrow the difference in absorbed bacteria from different pore structure and alkalinity of RCA and RBA, thus promoting the similar amount of precipitates formed, but the effect on the decrease in water absorption was not consistent.

3.7. XRD

Fig. 13 showed the X-ray diffraction patterns of RCA and RBA under basic MICP treatment and SA-aided MICP treatment, which was mainly applied to qualitatively test their mineral composition. Calcite and vaterite are the two most common crystal forms of $CaCO_3$ [33], and calcite is the most stable crystal form. It can be seen that the characteristic peak of the precipitates was mainly distributed at 29.75°, which was calcite. The second and third strongest characteristic peaks were vaterite at around 26.98° and 32.72°. The crystallinity in XRD is related to peak strength/peak width. Specifically, the area of the peak indicates the crystal content, and the larger the area, the higher the crystal phase content.

Under basic MICP treatment, calcite is the most crystalline form of the precipitates, followed by vaterite. Under SA-aided MICP treatment, similar results could be found that the crystal forms of the precipitates in both RCA-SA group and RBA-SA group were mainly calcite, followed by the vaterite. However, the difference was that the peak strength of calcite in RCA -Basic group was higher than that in RBA-Basic group and the peak strength of calcite in RCA-SA group was also higher than that in RBA-SA group. Furthermore, the peak strength of vaterite in RCA-Basic group was lower than that in RBA-basic group, and the peak strength of vaterite in RCA-SA group was also lower than that in RBA-SA group. There were two reasons for this difference. On the one hand, due to high porosity, there were more bacteria adhered to RBA than RCA, it implied that the urease activity in the RBA groups were higher. The urea decomposition in RBA groups was thus higher than that in RCA groups, and the precipitation rate in RBA groups was faster than that in RCA groups. Rapid precipitation rate tends to form more vaterite and less calcite [34]. On the other hand, the alkalinity of RCA is higher than RBA, and the formation of $CaCO_3$ crystals under various pH conditions have some differences, which has been reported that the content of calcite increases with the increase of pH value during the deposition of calcium carbonate [33]. In addition, for RBA, the peak strength of calcite in RBA-Basic group was apparently higher than that in RBA-SA group. This was due to the fact that SA-aided MICP treatment could absorb large amount of bacteria, thus promoting more urea decomposition and accelerating the precipitation rate, resulting in formation of more vaterite and less calcite. Overall, the differences in calcium carbonate crystal types in this study primarily due to the difference in the precipitation rate. Variations in pore property, alkalinity, and different MICP treatment methods led to differences in the amount of bacteria adhered to the aggregates and in urease activity, which in turn affected the precipitation rate, resulting in differences in the types of calcium carbonate crystals.

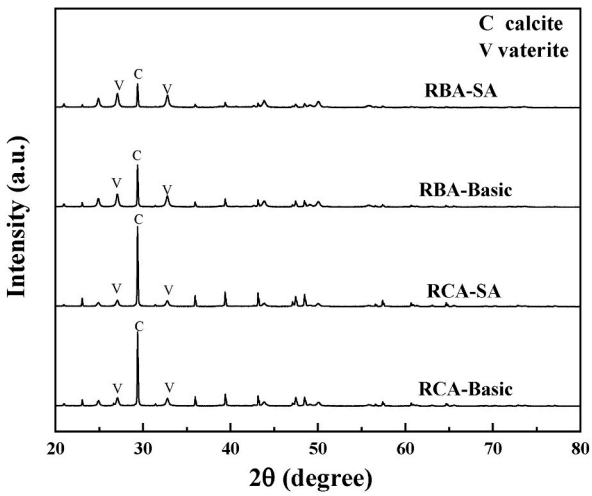

Fig. 13. The XRD of RCA and RBA after basic MICP treatment and SA-aided MICP treatment.

3.8. TGA

Fig. 14 showed the TG-DSC curves of the precipitates on RCA and RBA under basic MICP treatment and SA-aided MICP treatment. Calcium carbonate decomposes thermally into calcium oxide and carbon dioxide at the temperature range of 650–800 °C [35], so $CaCO_3$ can be identified from the characteristic endothermic peaks in Fig. 14. As illustrated in Fig. 14(a), the characteristic endothermic peak of $CaCO_3$ decomposition of RCA subjected to basic MICP treatment was at 760 °C, and the characteristic endothermic peak of RCA-SA group shifted to the right, 749 °C. The change of characteristic peak position was mainly resulted from the presence of unstable forms of $CaCO_3$, such as amorphous or the polymorphs vaterite, as well as the aragonite [36]. The weight loss during 650–800 °C of RCA-Basic and RCA-SA groups were 42.1 % and 40.8 %, respectively, and the $CaCO_3$ contents could be calculated according to the weight loss during the temperature range of $CaCO_3$ decomposition. The $CaCO_3$ content of RCA-Basic group was 95.7 %, which was slightly higher than that of RCA-SA group, 92.7 %. It might be that the precipitates in RCA-SA group contained a small account of Ca-alginate. As for RBA in Fig. 14(b), the characteristic endothermic peak of occurred at 751 °C and 743 °C. The weight loss during 650–800 °C of RBA-Basic and RBA-SA groups were 42.0 % and 41.1 %, respectively, thus the $CaCO_3$ contents of them were 95.5 % and 93.4 %, respectively.

3.9. Morphology of the precipitates

Fig. 15 Fig. 16, and Fig. 17 showed the surface morphology of RCA. As for the untreated RCA in Fig. 15(a) and (b), it could be observed an apparent micro-crack, with the crack width of around 2–5 μm, and some micropores (about 2–5 μm) were on the surface. After basic MICP treatment in Fig. 16(a) and (b), the $CaCO_3$ formed on the surface were square and irregular in shape, with a size of around 5–10 μm. As shown in Fig. 17(a), after SA-aided MICP treatment, some sphere $CaCO_3$ with the size of 5–20 μm were formed on the surface of RCA, and a large number of bacterial imprints could be observed on the $CaCO_3$. Moreover, it was found in Fig. 17(a) that the Ca-alginate sheet could be observed, which was caused by drying. Calcium carbonate formed on the Ca-alginate sheet, indicating that this is a composite coating precipitation. Therefore, for SA-aided MICP treatment, it is necessary to increase the amount of $CaCO_3$ and minimize the amount of Ca-alginate.

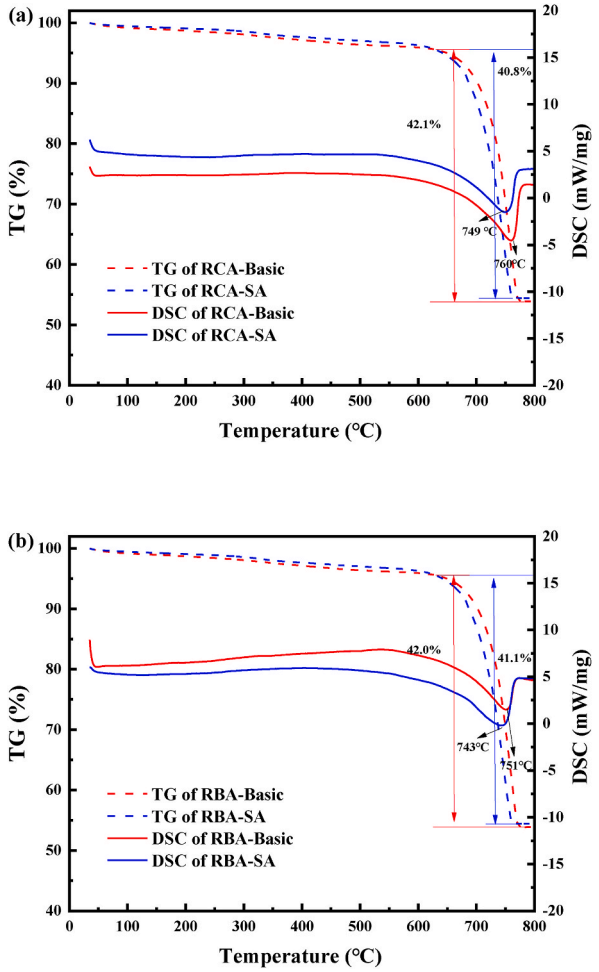

Fig. 14. TD-DSC curves of (a) RCA and (b) RBA under basic MICP treatment and SA-aided MICP treatment.

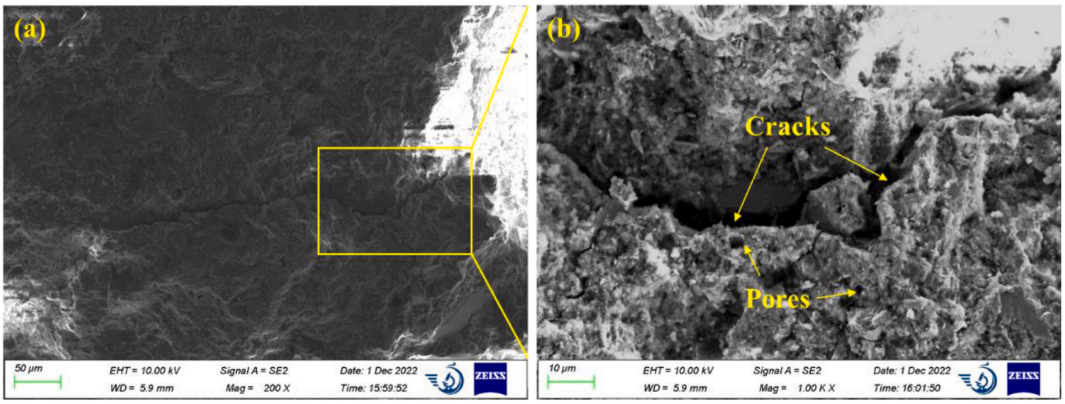

Fig. 15. SEM images of untreated RCA.

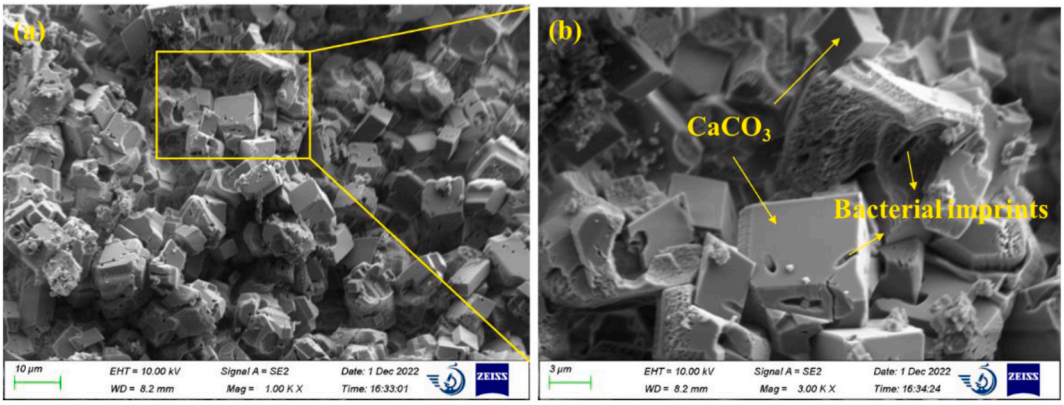

Fig. 16. SEM images of RCA treated by basic MICP treatment.

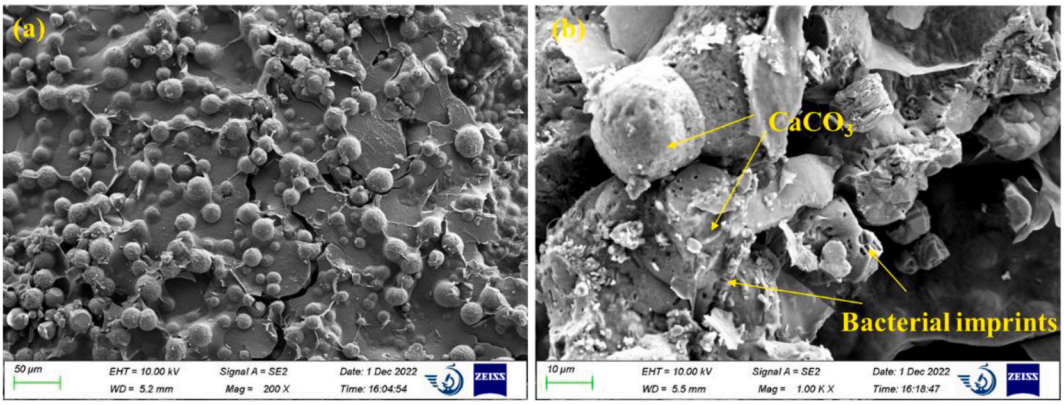

Fig. 17. SEM images of RCA treated by SA-aided MICP treatment.

As for RBA, in Fig. 18 (a) and (b), the sizes of micropores (about 30 μm) and microcracks (about 50 μm) were significantly larger than that of RCA. In Fig. 19 (a), after basic MICP treatment, the $CaCO_3$ formed on the surface were square and irregular in shape, with a size of around 5–10 μm. Some bacterial imprints could be observed on the RBA surface bio-treated by basic MICP treatment in Fig. 19 (b). Differently, after SA-aided MICP treatment in Fig. 20 (a), the $CaCO_3$ precipitates were relatively rough and not only sphere, but also in shape of square and irregular. Moreover, large quantities of bacterial imprints could be found in Fig. 20 (b), which indicated that Ca-alginate network formed could encapsulate a large number of bacteria on the aggregates. Additionally, it was shown in Fig. 20 (a), there was no obvious Ca-alginate sheet, but more calcium carbonate precipitation comparing with Fig. 17(a), indicating that the aggregates in RBA-SA group adsorbed more bacteria than that in RCA-SA group, thus decomposing more urea and inducing more

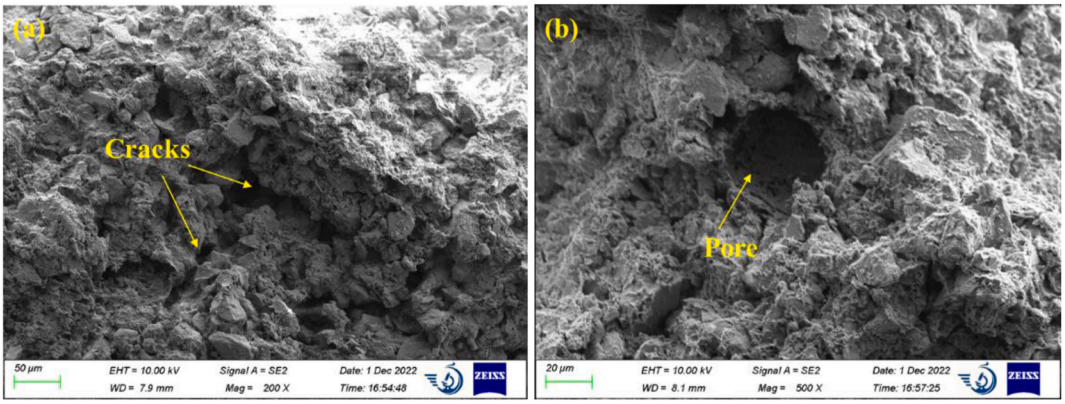

Fig. 18. SEM images of untreated RBA.

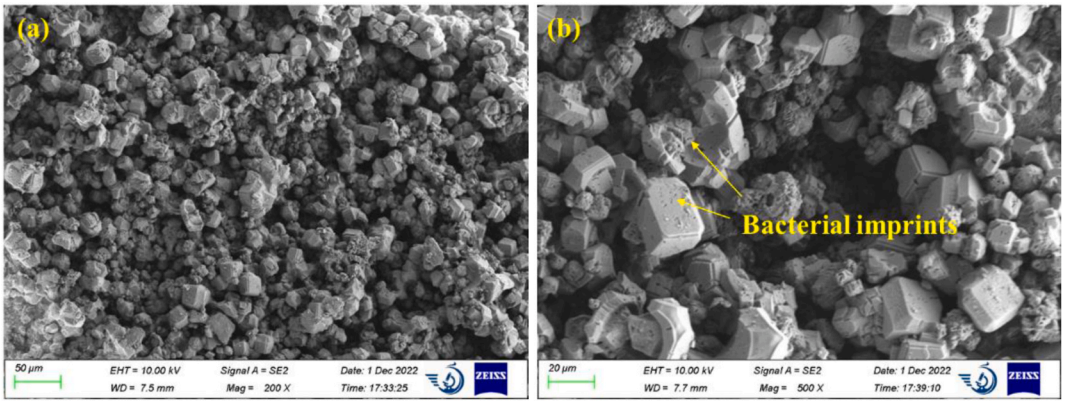

Fig. 19. SEM images of RBA treated by basic MICP treatment.

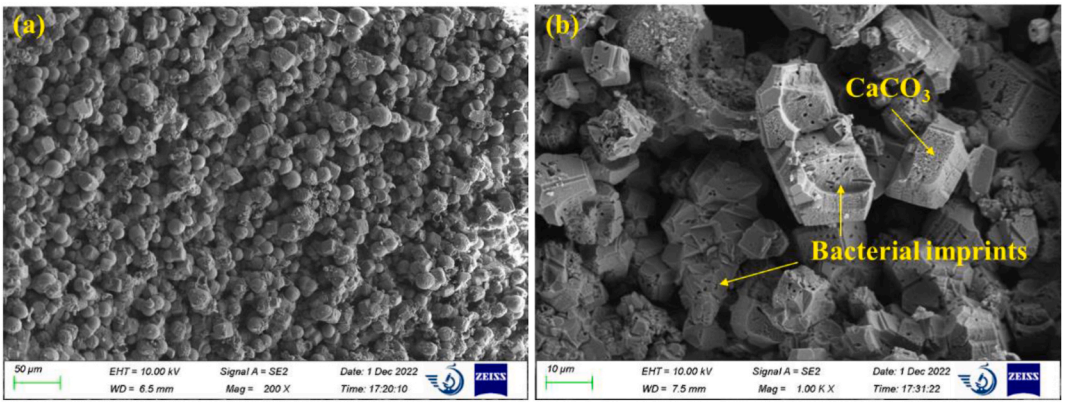

Fig. 20. SEM images of RBA treated by SA-aided MICP treatment.

$CaCO_3$ precipitates.

3.10. MIP

Fig. 21 showed the porosity and pore size distribution of aggregates with untreated, SA-aided, and basic MICP treatment. It can be found in Fig. 21(a) that there was a significantly difference of porosity on untreated RCA and RBA, and the total porosities of them were respectively 28.3 % and 40.7 % according to the MIP results. After basic MICP treatment, the porosity of RCA and RBA were reduced to 20.4 % and 28.5 %, respectively. After SA-aided MICP treatment, the porosities of RCA and RBA were reduced to 14.8 % and 21.4 %, respectively, which was significantly lower than the porosity of aggregates under basic MICP treatment.

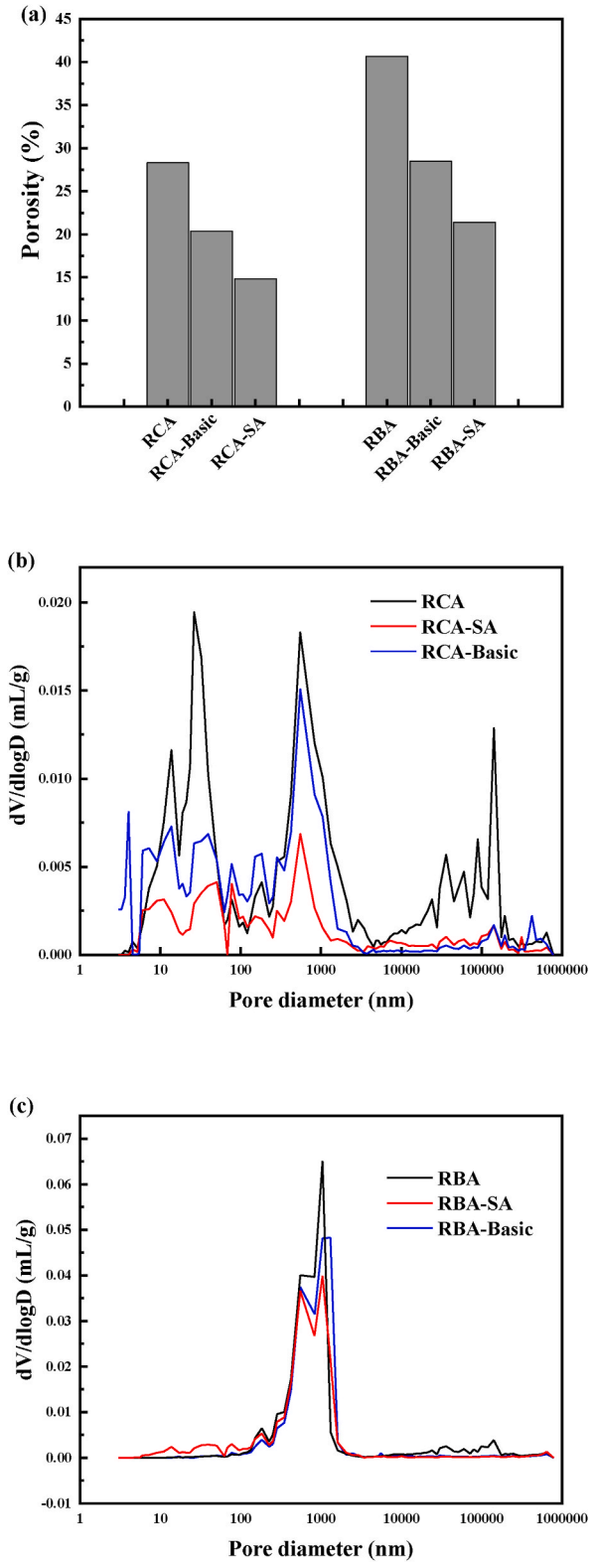

Fig. 21. The (a) porosity and pore size distribution of (b) RCA and (c) RBA under different MICP treatments.

As illustrated in Fig. 21(b), the pore size of untreated RCA was mainly less than 1 μm (micropore), and some of them were around 100 μm (large pores). After basic MICP treatment and SA-aided MICP treatment, the porosities of RCA were significantly decreased, especially the micropores of 100 μm, which might be because large pores were more readily occupied by bacteria and induce the formation of $CaCO_3$ [23]. As shown in Fig. 21(c), the pore size distribution of RBA was primarily situated around 1000 nm, and the highest distribution peak could reach to 0.065 mL/g, significantly larger than RCA, approximately 0.02 mL/g. Some of pores were also distributed at 100 μm, and the peak of large pore was completely disappeared after MICP treatment, which was similar with the results of above Fig. 21(b). Due to the formation of $CaCO_3$ after SA-aided MICP treatment, the highest peak of RBA was decreased to 0.04 mL/g, and as for RCA in Fig. 19(b), the highest peak of pore size distribution was decreased from around 0.02 to 0.005 mL/g, which indicated that SA-aided MICP treatment was more conducive to decrease the porosities of RCA and RBA, as well as refining the pore size distribution than that of basic MICP treatment.

The difference in physical property between RCA and RBA was the pore structure characteristics, such as porosity and pore size distribution, which significantly affect the formation of biogenic $CaCO_3$ [37]. The formation of biogenic $CaCO_3$ depends on the catalysis of ureolytic bacteria, and more bacteria and higher urease activity can decompose more urea to produce more carbonate ions, thus generating more biogenic $CaCO_3$. RBA with high porosity tends to absorb more bacteria than RCA, resulting in higher urea decomposition in the precipitation process, and higher mass increase. Also in Fig. 19(a), it can be found that the porosity of RBA was significantly larger than RCA, and some micropores (less than 100 nm) were appeared in RCA. It has been found that biogenic crystals were preferential generated around and inside open pores, including surface large pores and micro-cracks [38]. This may be because large pores and micro-cracks were more likely to be occupied by bacteria acting as nucleation sites and thus repaired by the biogenic $CaCO_3$.

The function of using sodium alginate (SA) is to encapsulate bacteria on aggregates through the formed Ca-alginate network structure when exposed to calcium, promote the in-situ formation of biogenic $CaCO_3$ on the aggregates, and achieve complete repair of the entire surface of aggregates [24]. Compared with the basic MICP treatment, the SA-aided treatment was focused on the surface repairment, which could be found in Fig. 21(b) and (c) that the surface visible pores (larger than 100 μm) were almost completely repaired under SA-aided treatment. Therefore, for the difference in pore structure and alkalinity between RCA and RBA, SA-aided MICP treatment could effectively reduce the impact of these differences on treatment efficiency to a certain extent.

4. Conclusions

In this research, it was demonstrated that pore structure and alkalinity had an important influence on the bio-deposition treatment efficiency of recycled aggregates. The specific conclusions are as follows.

(1) Due to higher porosity of RBA and the more suitable alkalinity for bacteria, after absorption and desorption processes, the bacteria adhered on RBA was much higher than that on RCA. The adhered bacteria on aggregates were increased by more than 2 times under basic MICP treatment and more than 3 times under SA-aided MICP treatment. From the perspective of efficiency of MICP treatments, compared with RCA, the more bacteria adhered to RBA with high porosity and more suitable alkalinity, the more quantities of $CaCO_3$ generated, and the more significant decrease in water absorption.
(2) For both RCA and RBA, the quantities of formed $CaCO_3$ under SA-aided MICP treatment was higher and more uniform than that under basic MICP treatment, and the corresponding water absorption decreases more significantly. The maximum decrease in water absorption (46.02 % on average) occurred in RBA-SA group.
(3) Under SA-aided MICP treatment, the influence of pore structure and alkalinity of aggregates on the treatment efficiency was not significant compared with that under the basic MICP treatment, especially the mass of $CaCO_3$ on the aggregates. This concluded that SA-aided treatment could weaken the influence of pore structure and alkalinity from different aggregates on the amount of formed biogenic precipitates, which was conducive to the unified application of SA-aided MICP treatment on different types of recycled aggregates.

CRediT authorship contribution statement

Jianyun Wang: Writing – review & editing, Writing – original draft, Supervision, Methodology, Funding acquisition, Data curation, Conceptualization. **Rui Zhang:** Writing – review & editing, Writing – original draft, Methodology, Investigation, Conceptualization. **Fuxing Hou:** Methodology, Investigation, Data curation. **Guang Ye:** Investigation, Formal analysis, Data curation.

Declaration of competing interest

We declare that we have no financial and personal relationships with other people or organizations that can inappropriately influence our work, there is no professional or other personal interest of any nature or kind in any product, service and/or company that could be construed as influencing the position presented in, or the review of, the manuscript entitled.

Data availability

Data will be made available on request.

Acknowledgements

This work was supported by the National Natural Science Foundation of China (No.51908459 and No.52178252); and 'Young Talent Support Plan' of Xi'an Jiaotong University.

References

[1] N.S. Reddy, M. Lahoti, A succinct review on the durability of treated recycled concrete aggregates, Environ Sci Pollut R (2022), https://doi.org/10.1007/s11356-021-18168-w.
[2] R.V. Silva, J. de Brito, R.K. Dhir, Use of recycled aggregates arising from construction and demolition waste in new construction applications, J. Clean. Prod. 236 (2019), https://doi.org/10.1016/j.jclepro.2019.117629.
[3] M. Amin, B.A. Tayeh, I.S. Agwa, Effect of using mineral admixtures and ceramic wastes as coarse aggregates on properties of ultrahigh-performance concrete, J. Clean. Prod. 273 (2020), https://doi.org/10.1016/j.jclepro.2020.123073.
[4] J.Z. Xiao, Z.M. Ma, T.B. Sui, A. Akbarnezhad, Z.H. Duan, Mechanical properties of concrete mixed with recycled powder produced from construction and demolition waste, J. Clean. Prod. 188 (2018) 720–731, https://doi.org/10.1016/j.jclepro.2018.03.277.
[5] F. Aslani, G.W. Ma, D.L.Y. Wan, G. Muselin, Development of high-performance self-compacting concrete using waste recycled concrete aggregates and rubber granules, J. Clean. Prod. 182 (2018) 553–566, https://doi.org/10.1016/j.jclepro.2018.02.074.
[6] H. Guo, C. Shi, X. Guan, J. Zhu, Y. Ding, T.-C. Ling, H. Zhang, Y. Wang, Durability of recycled aggregate concrete–A review, Cement Concrete Comp 89 (2018) 251–259, https://doi.org/10.1016/j.cemconcomp.2018.03.008.
[7] A. Akhtar, A.K. Sarmah, Construction and demolition waste generation and properties of recycled aggregate concrete: a global perspective, J. Clean. Prod. 186 (2018) 262–281, https://doi.org/10.1016/j.jclepro.2018.03.085.
[8] J.H. Zhang, L. Ding, F. Li, J.H. Peng, Recycled aggregates from construction and demolition wastes as alternative filling materials for highway subgrades in China, J. Clean. Prod. 255 (2020), https://doi.org/10.1016/j.jclepro.2020.120223.
[9] F.D. Salgado, F.D. Silva, Recycled aggregates from construction and demolition waste towards an application on structural concrete: a review, J. Build. Eng. 52 (2022), https://doi.org/10.1016/j.jobe.2022.104452.
[10] J. Sivamani, N.T. Renganathan, S. Palaniraj, Enhancing the quality of recycled coarse aggregates by different treatment techniques-a review, Environ Sci Pollut R 28 (43) (2021) 60346–60365, https://doi.org/10.1007/s11356-021-16428-3.
[11] W. Wei, Z.S. Shao, R.J. Qiao, W.W. Chen, H. Zhou, Y. Yuan, Recent development of microwave applications for concrete treatment, Constr Build Mater 269 (2021), https://doi.org/10.1016/j.conbuildmat.2020.121224.
[12] W. Wei, Z.S. Shao, Y.Y. Zhang, R.J. Qiao, J.P. Gao, Fundamentals and applications of microwave energy in rock and concrete processing - a review, Appl. Therm. Eng. 157 (2019), https://doi.org/10.1016/j.applthermaleng.2019.113751.
[13] J.A. Forero, J.D. Brito, L. Evangelista, C. Pereira, Improvement of the quality of recycled concrete aggregate subjected to chemical treatments: a review, Materials 15 (8) (2022), https://doi.org/10.3390/ma15082740.
[14] M.J. Munir, S.M.S. Kazmi, Y.F. Wu, X.S. Lin, Axial stress-strain performance of steel spiral confined acetic acid immersed and mechanically rubbed recycled aggregate concrete, J. Build. Eng. 34 (2021), https://doi.org/10.1016/j.jobe.2020.101891.
[15] H. Katkhuda, N. Shatarat, Improving the mechanical properties of recycled concrete aggregate using chopped basalt fibers and acid treatment, Constr Build Mater 140 (2017) 328–335, https://doi.org/10.1016/j.conbuildmat.2017.02.128.
[16] J. Zhang, C. Shi, Y. Li, X. Pan, C.-S. Poon, Z. Xie, Performance enhancement of recycled concrete aggregates through carbonation, J Mater Civil Eng 27 (11) (2015) 04015029, https://doi.org/10.1061/(ASCE)MT.1943-5533.0001296.
[17] L. Li, D. Xuan, A.O. Sojobi, S. Liu, S. Chu, C.S. Poon, Development of nano-silica treatment methods to enhance recycled aggregate concrete, Cement Concrete Comp 118 (2021) 103963, https://doi.org/10.1016/j.cemconcomp.2021.103963.
[18] R. Zhang, K. Wu, Z.W. Jiang, J.Y. Wang, Bacterially induced CaCO3 precipitation for the enhancement of quality of coal gangue, Constr Build Mater 319 (2022), https://doi.org/10.1016/j.conbuildmat.2021.126102.
[19] A.M. Grabiec, J. Klama, D. Zawal, D. Krupa, Modification of recycled concrete aggregate by calcium carbonate biodeposition, Constr Build Mater 34 (2012) 145–150, https://doi.org/10.1016/j.conbuildmat.2012.02.027.
[20] J.Y. Wang, B. Vandevyvere, S. Vanhessche, J. Schoon, N. Boon, N. De Belie, Microbial carbonate precipitation for the improvement of quality of recycled aggregates, J. Clean. Prod. 156 (2017) 355–366, https://doi.org/10.1016/j.jclepro.2017.04.051.
[21] J. Wang, H.M. Jonkers, N. Boon, N. De Belie, Bacillus sphaericus LMG 22257 is physiologically suitable for self-healing concrete, Appl Microbiol and Biot 101 (12) (2017) 5101–5114, https://doi.org/10.1007/s00253-017-8260-2.
[22] J. Wang, B. Vandevyvere, S. Vanhessche, J. Schoon, N. Boon, N. De Belie, Microbial carbonate precipitation for the improvement of quality of recycled aggregates, J. Clean. Prod. 156 (2017) 355–366, https://doi.org/10.1016/j.jclepro.2017.04.051.
[23] K. Liu, J. Ouyang, D. Sun, N. Jiang, A. Wang, N. Huang, P. Liang, Enhancement mechanism of different recycled fine aggregates by microbial induced carbonate precipitation, J. Clean. Prod. 379 (2022) 134783, https://doi.org/10.1016/j636.jclepro.2022.134783.
[24] R. Zhang, K. Wu, D. Xie, J. Wang, Using sodium alginate aided bio-treatment for improving the uniformity of precipitates on recycled aggregates, Appl Microbiol Biot 107 (5) (2023) 1525–1536, https://doi.org/10.1007/s00253-023-12394-7.
[25] B. Standard, Aggregates for concrete, BS EN (2002) 12620.
[26] R. Zhang, D. Xie, K. Wu, J. Wang, Optimization of sodium alginate aided bio-deposition treatment of recycled aggregates and its application in concrete, Cement Concrete Comp 139 (2023) 105031, https://doi.org/10.1016/j.cemconcomp.2023.105031.
[27] G.R. Morrison, Microchemical determination of organic nitrogen with Nessler Reagent, Anal. Biochem. 43 (2) (1971) 527, https://doi.org/10.1016/0003-2697(71)90283-1.
[28] R. Zhang, J. Wang, Effect of regulating urease activity on the properties of bio-CaCO3 precipitated on recycled aggregates, Constr Build Mater 403 (2023) 133119, https://doi.org/10.1016/j.conbuildmat.2023.133119.
[29] B. Mortensen, M. Haber, J. DeJong, L. Caslake, D. Nelson, Effects of environmental factors on microbial induced calcium carbonate precipitation, J. Appl. Microbiol. 111 (2) (2011) 338–349, https://doi.org/10.1111/j.1365-2672.2011.05065.x.
[30] H. Choi, M. Inoue, R. Sengoku, Change in crystal polymorphism of CaCO3 generated in cementitious material under various pH conditions, Constr Build Mater 188 (2018) 1–8, https://doi.org/10.1016/j.conbuildmat.2018.08.045.
[31] M.A. Imran, K. Nakashima, N. Evelpidou, S. Kawasaki, Factors affecting the urease activity of native ureolytic bacteria isolated from coastal areas, Geomech, Eng 17 (5) (2019) 421–427, https://doi.org/10.12989/gae.2019.17.5.421.
[32] M. Fujita, K. Nakashima, V. Achal, S. Kawasaki, Whole-cell evaluation of urease activity of Pararhodobacter sp. isolated from peripheral beachrock, Biochem. Eng. J. 124 (2017) 1–5, https://doi.org/10.1016/j.bej.2017.04.004.
[33] A. Ali, M. Li, J. Su, Y. Li, Z. Wang, Y. Bai, E.F. Ali, S.M. Shaheen, Brevundimonas diminuta isolated from mines polluted soil immobilized cadmium (Cd2+) and zinc (Zn2+) through calcium carbonate precipitation: microscopic and spectroscopic investigations, Sci. Total Environ. 813 (2022) 152668, https://doi.org/10.1016/j578.scitotenv.2021.152668.
[34] K.A. Gebru, T.G. Kidanemariam, H.K. Gebretinsae, Bio-cement production using microbially induced calcite precipitation (MICP) method: a review, Chem. Eng. Sci. 238 (2021) 116610, https://doi.org/10.1016/j.ces.2021.116610.
[35] M. Li, X. Zhu, A. Mukherjee, M. Huang, V. Achal, Biomineralization in metakaolin modified cement mortar to improve its strength with lowered cement content, J. Hazard Mater. 329 (2017) 178–184, https://doi.org/10.1016/j.jhazmat.2017.01.035.

[36] M. Nedeljković, J. Visser, T.G. Nijland, S. Valcke, E. Schlangen, Physical, chemical and mineralogical characterization of Dutch fine recycled concrete aggregates: a comparative study, Constr Build Mater 270 (2021) 121475, https://doi.org/10.1016/j.conbuildmat.2020.121475.
[37] W. De Muynck, S. Leuridan, D. Van Loo, K. Verbeken, V. Cnudde, N. De Belie, W. Verstraete, Influence of pore structure on the effectiveness of a biogenic carbonate surface treatment for limestone conservation, Appl Environ Microb 77 (19) (2011) 6808–6820, https://doi.org/10.1128/AEM.00219-11.
[38] D.V. Zamarreño, R. Inkpen, E. May, Carbonate crystals precipitated by freshwater bacteria and their use as a limestone consolidant, Appl Environ Microb 75 (18) (2009) 5981–5990, https://doi.org/10.1128/AEM.02079-08.